Int. J. Plant Sci. 166(5):723–732. 2005.

1058-5893/2005/16605-0004$15.00

AUTOMATED IMAGE ANALYSIS OF ANNUAL RINGS IN THE ROOTS OF PERENNIAL FORBS

Georg von Arx[1] and Hansjoerg Dietz

Geobotanical Institute, Swiss Federal Institute of Technology, Zürichbergstrasse 38, 8044 Zürich, Switzerland

Analysis of annual rings in the secondary root xylem is a relatively new approach to gain a posteriori insight into individual and population life history of perennial dicotyledonous herbs (herb-chronology). Until now, herb-chronology has involved manual analysis, which is limited by low reproducibility and comparability and which requires considerable time and expertise from the researcher. We have therefore developed an automated image analysis system (Root Xylem Analysis System [ROXAS]) to improve the standardization and efficiency of conventional herb-chronological analysis. Digital images of stained root cross sections are used by ROXAS to automatically extract xylem vessels according to morphometric criteria. Annual rings are detected by pattern algorithms that analyze the local anatomical context of each vessel. Besides growth parameters, such as annual ring width and area, parameters related to functional root anatomy, such as vessel area or vessel density, are automatically calculated. We evaluated the results produced by ROXAS, using six individuals from each of five perennial plant species representing a variety of taxonomic groups and anatomical root patterns. All species were conducive to automated analysis, which was six times faster than the manual method. Overall, 95% of all annual rings and 98% of all vessels were correctly identified. Accuracy of automated ring width measurements tended to be slightly higher than that of manual analysis, ranging from 2.1% to 5.3% deviation from reference data for all species. Further anatomical parameters, such as vessel area or vessel density, varied substantially between species, indicating anatomical adaptations of these perennial forbs to the constraints of their specific habitats. Automated herb-chronology using ROXAS may therefore prove to be useful for efficient and reproducible analysis of annual growth increments in the roots of forbs and for investigations into their functional root anatomy.

Keywords: annual rings, annual ring width, automated image analysis, forbs, herb-chronology, pattern recognition, vessel density, vessel area, xylem vessels.

Introduction

The growth and life history of perennial forbs often extends over a much longer period of time than those of annuals. Therefore, it is important to know the long-term developmental trajectories of perennial plants (individuals and populations) to understand their biology and ecology in the environmental context (Harper 1977; Roach 2003). The analysis of annual rings in the secondary root xylem is a rather new approach to gaining a posteriori insight into the life history of individuals and populations of perennial dicotyledonous herbs (herb-chronology; Humulum 1981; Boggs and Story 1987; Dietz and Ullmann 1997; Dietz and Fattorini 2002; Dietz and Schweingruber 2002).

The anatomical bases of discernible annual rings in the secondary root xylem of forbs are the formation of earlywood vessels with wide lumina in spring and the development of latewood vessels with narrower lumina in late summer and autumn (Werner 1978; Boggs and Story 1987; Dietz and Ullmann 1997). In woody plants, a comparable anatomical pattern is termed, depending on its distinctness, ring- or semi-ring-porous anatomy (Carlquist 2001). In a few forb species, variation in vessel size is not very pronounced, but there is often a decrease in vessel density from earlywood to latewood (diffuse porous pattern) that helps to identify annual rings (Carlquist 2001).

Annual rings in forbs can be used not only for age determination but also for evaluation of plant growth patterns by analysis of the variation in annual ring width. Recent studies have demonstrated that variations in annual ring width correlate with variations in environmental growth conditions (e.g., temperature, light, competition; Dietz and Ullmann 1998; Dietz and Fattorini 2002; Dietz et al. 2004; Dietz and von Arx 2005).

Until now, annual rings in the roots of perennial forbs have been analyzed manually using digital images of root cross sections. Plant age, the most basic information preserved in annual rings, has been determined by counting annual rings along a given radius. In this straightforward approach, problems have arisen if ring demarcation has not been clear on the chosen radius. In such instances, tangential cross-comparisons with other radii may have helped. Ring width has been determined manually on three representative radii using linear measurement tools in appropriate technical drawing or image analysis software (Dietz and Fattorini 2002; Dietz and von Arx 2004, 2005; Dietz et al. 2004). Means of the three measurements have been used as the

[1] E-mail georg.vonarx@env.ethz.ch.

Manuscript received November 2004; revised manuscript received April 2005.

width of the respective rings (Dietz and Fattorini 2002; Dietz et al. 2004). If radial growth is asymmetric around the root, this approach may lead to large errors in the estimation of ring width and inconsistencies between different observers (Soille and Misson 2001).

Automation of herb-chronological procedure may reduce the limitations of manual analysis by rendering the analysis more accurate and objective and improving comparability among researchers working on the same taxonomic group. Automation may also help to make the use of herb-chronology more efficient and provide training and increased accessibility for inexperienced users. Hence, automation may facilitate a more widespread use of herb-chronology. In addition, automation can enhance the potential of herb-chronology by expanding the set of measurable parameters to those related to functional root anatomy.

Several image analysis software packages are available for studying annual rings in woody plants (dendrochronology). To our knowledge, all these packages use wood density or light intensity variations to identify annual rings (Grissino-Mayer 1996; Grissino-Mayer and Fritts 1997; Conner et al. 2000; Soille and Misson 2001). These two parameters generally do not apply to roots of perennial forbs, since many forbs show lignification only in the cell walls of the vessels and fluctuating light intensities often represent only irregularly occurring rings of lignified parenchyma cells (Rabotnov 1960; Werner 1978). Thus, identification of annual rings in perennial forbs is best based on vessel size and distribution patterns of vessels in the secondary xylem (Dietz and Ullmann 1997; Dietz and Schweingruber 2002).

Here we present the vessel-based automated analysis system ROXAS (Root Xylem Analysis System). We have designed ROXAS to detect xylem vessels automatically, identify and measure annual rings, determine plant age, and provide additional anatomical parameters, such as vessel density or vessel size, in root cross sections of perennial forbs. This article describes the conceptual framework and functioning of ROXAS and evaluates its accuracy in vessel extraction, identification of annual rings, and annual ring width measurement. Therefore, five perennial forb species from four different families of the temperate climate zone were analyzed. We also outline the more general potential of providing vessel-based anatomical parameters for investigations into the functional ecology of perennial forbs.

Material and Methods

Data Collection

Root sampling and processing. Five species of perennial forbs were selected for analysis by ROXAS. Species were selected to represent a variety of taxonomic groups and anatomical root patterns (table 1; fig. 1). In addition, the plants were sampled across a wide altitudinal gradient. All plants grew in open, unshaded herbaceous vegetation in mesic habitats. For each species, 10–30 well-established individuals were randomly selected. For the plants sampled from a common garden experiment (table 1), the oldest available plants (4 yr old) were selected.

The roots of the plants were carefully excavated and cut near the proximal end (root collar) to avoid missing annual rings (Dietz and Fattorini 2002). Using a sledge microtome, thin cross sections (20–35 μm) were produced. The cross sections of the roots were stained with Phloroglucinol/HCl (causing reddish coloration of the cell walls of vessels and lignified parenchyma cells) and examined under a dissecting microscope (Leica MZ 8). Cross sections were photographed through the receptacle tube of the microscope using a digital camera (Nikon CoolPix 990, resolution 2048×1536 pixels). A copper wire (diameter 50 μm) was placed at the side of each cross section as a scale reference.

Data processing and determination of annual ring width. For each species, three plants with representative anatomies were used for initial calibration of ROXAS (see below), and six different, randomly chosen plants were used for evaluation. From each cross section, the largest coherent sector of the secondary xylem available in the digital image was used for analysis (fig. 2*a*). Sector size ranged from 80° to 130°. Three different analysis methods were applied to each cross section: (i) manual measurements of annual ring widths with the line tool of Media Cybernetics Image-Pro Plus along three representative radii—means of the three measurements were used as the respective annual ring widths (hereafter termed "manual analysis"); (ii) manually tracing the outline

Table 1

Characterization of the Sampling Sites and Anatomical Patterns in the Study Species

Species	Family	Site, habitat	Altitude (m a.s.l.)	Location	Zonal pattern[a]
Bunias orientalis	Brassicaceae	Achau, ruderal roadside	200	48°04′N, 16°23′E	VL, VB, [PZ]
B. orientalis	Brassicaceae	St. Maurice, ruderal roadside	600	46°12′N, 7°00′E	VL, VB, [PZ]
Erinus alpinus	Scrophulariaceae	Alpstein Mountains, rock wall	1500–1900	47°15′N, 9°20′E	[VL], VD, PC
Penstemon venustus	Scrophulariaceae	Southeast Wallowa Mountains, open slopes	1350–2000	45°N, 117°W	VL, VD, PI
Sanguisorba minor	Rosaceae	Zürich, common garden experiment	500	47°22′N, 8°31′E	VL, PI
Trifolium badium	Fabaceae	Northern Swiss Alps, alpine grassland	2000–2200	46°50′N, 8°E	VL, VD

Note. All sites except for the Wallowa Mountains (northeast Oregon) and Achau (Austria) are located in Switzerland.

[a] VL = differential vessel lumina; VD = differential vessel density; VB = zonal branching of vessel rays; PZ = zonal lignification of parenchyma cells; PC = complete lignification of parenchyma cells; PI = zonal interruption of the completely lignified parenchyma. If an anatomical pattern was present in only a fraction of the analyzed individuals of a species, its abbreviation is given in brackets.

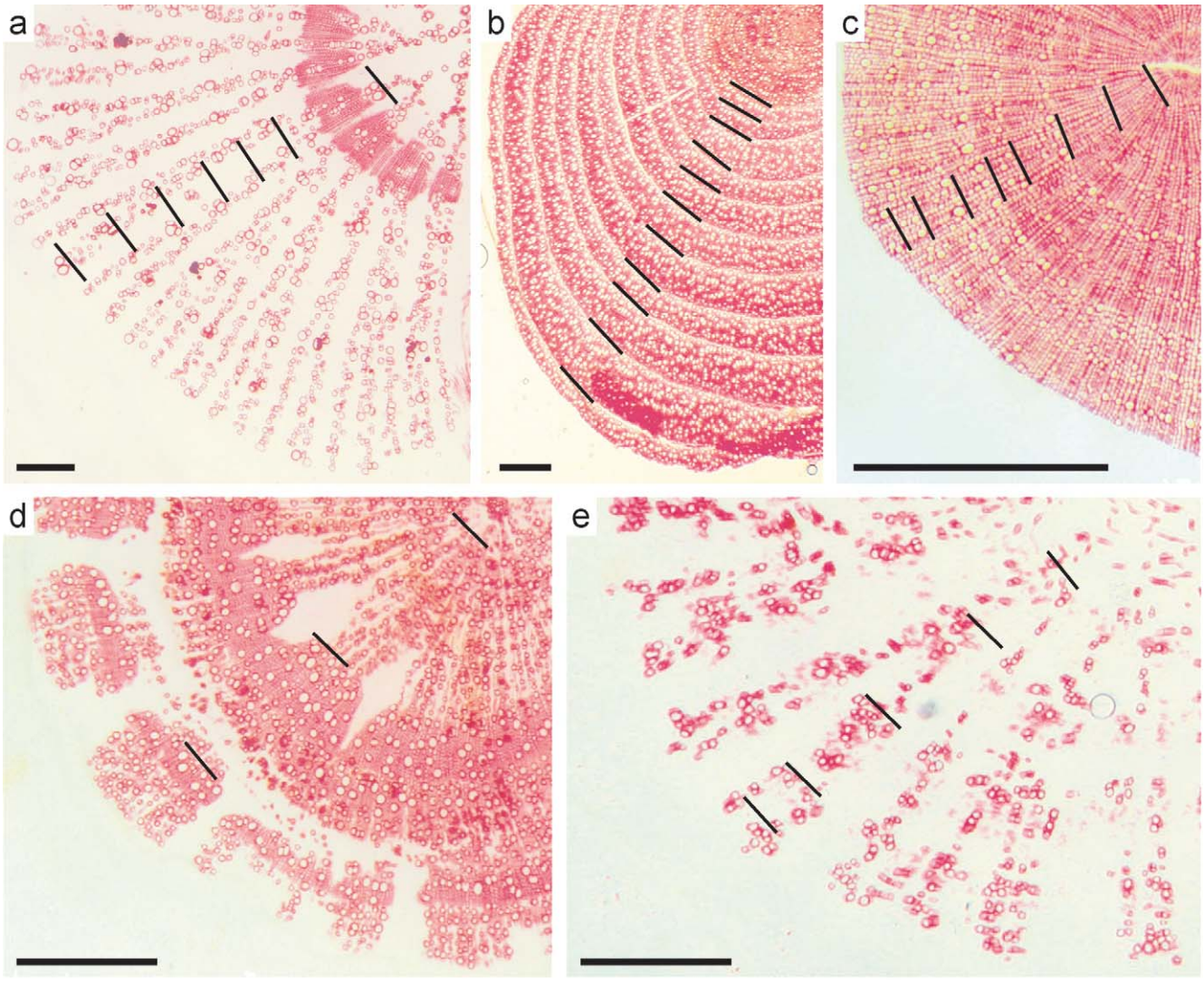

Fig. 1 Examples of anatomical patterns in the root xylem of (*a*) *Bunias orientalis*, (*b*) *Erinus alpinus*, (*c*) *Penstemon venustus*, (*d*) *Sanguisorba minor*, and (*e*) *Trifolium badium*, as viewed through a dissecting microscope. Lignified structures are stained with Phloroglucinol/HCl. The markers along the xylem radii denote transitions from latewood of the previous growing period to earlywood of the following one. Scale bars = 500 μm.

of each annual ring using the polygon tool of Image-Pro Plus—reference mean ring width was calculated based on the traced polygon area (hereafter termed "reference analysis"); and (iii) automated analysis with ROXAS (see below).

Automated Analysis

Overview. ROXAS has been developed in Microsoft Visual Basic as a shell program that controls two other involved programs, Image-Pro Plus and MS Excel. Before automated analysis, pixel-to-unit-length ratio is calibrated for each image using the reference scale (copper wire). The center of the cross section is set as the origin, or zero point. After spatial calibration, automated image analysis, using species-specific calibration sets that account for anatomical differences between the species (see below), involves three consecutive processes (fig. 3): (i) extraction of the vessels in the secondary root xylem, (ii) detection of the innermost vessels of each earlywood zone (earlywood border vessels [EBVs]), and (iii) identification of the borders of the annual rings. In addition, these ring identification processes yield a set of further anatomical parameters that may be used for analysis of functional root anatomy (table 3).

Image processing. In the first step of automated analysis, the color image (fig. 3*a*, 3*b*) is converted to a gray-scale image by weighting the different color channels according to their importance for optimal image contrast. This facilitates and accelerates image analysis without losing critical information. The contrast of vessel structures is improved by local contrast and edge enhancement filters (Media Cybernetics 2001; Russ 2002). Both filters also eliminate inhomogeneous illumination and improve imperfect image focus. As a result, a black-and-white image that represents a coarse preselection

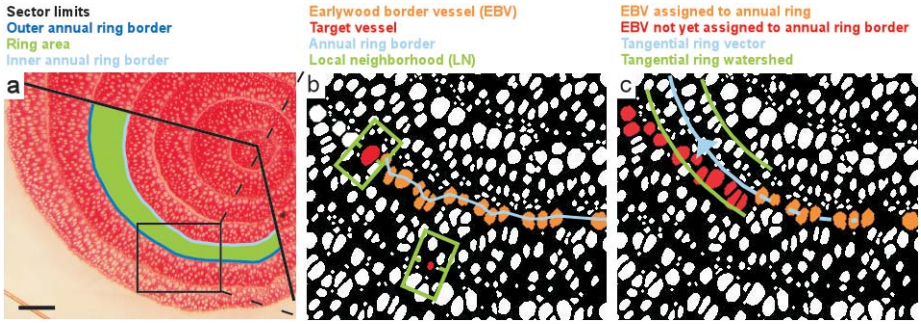

Fig. 2 Determination of ring width and area (*a*), pattern analysis for identification of earlywood border vessels (EBVs; *b*), and identification of annual rings (*c*) by ROXAS, as illustrated for a *Penstemon venustus* root section. *a*, Within the analyzed sector of the secondary xylem (delimited by the two black lines), the width of each annual ring is determined by subtracting the mean radius of the inner annual ring border (light blue) from the mean radius of the outer annual ring border (dark blue). Ring area (green) is calculated by subtracting a circle area with radius equivalent to the mean inner annual ring border (light blue) from a circle area with radius equivalent to the mean outer annual ring border (dark blue). *b*, In automated analysis, pattern recognition algorithms are applied to the local neighborhood (green windows) of each vessel. EBVs (light red and wide red target vessel) are identified by having narrower vessels in the inner (toward the root center) and similar sized vessels in the outer half of their local neighborhood. In contrast, non-EBVs (e.g., narrow red target vessel) show a rather homogeneous, isotropic local neighborhood of vessels. Annual ring borders (light blue) are identified by linearly connecting EBVs. *c*, Assignment of EBVs to the correct annual ring is achieved by a tangentially moving watershed area (between the green curves) centered on a ring vector (solid blue curve) that is projected based on already connected EBVs (see *b*). Only EBVs encountered within the moving watershed are assigned to the current annual ring border. Since the tangential ring vector dynamically changes direction based on the last few assigned EBVs, all not yet assigned EBVs (red) will be correctly included. Scale bar = 500 μm.

of xylem vessels (white objects) is obtained by intensity segmentation.

Vessel extraction. The black-and-white image contains many objects that are not true xylem vessels but lignified parenchyma cells and image noise (these objects are termed "pseudovessels" hereafter). To discriminate true vessels from pseudovessels, several morphometric parameters of the preselected objects are measured (see first row of table 2). The obtained parameter values are referenced to a species-specific calibration data set and weighted according to their importance in calculating a vessel index, which gives the likelihood of the extracted object's being a true vessel. A species-independent threshold of the vessel index is used to identify true vessels (fig. 3*c*). True vessels are usually wider and less angular than pseudovessels, and/or their ratio of major to minor axis is closer to 1 than that of pseudovessels.

Identification of earlywood borders and annual rings. Pattern recognition algorithms identify the innermost EBVs of each annual ring within the specified sector (fig. 2*a*) on the basis of the anatomical characteristics of each vessel's local neighborhood (fig. 2*b*; second row of table 2). The obtained parameter values are referenced to a species-specific calibration data set and weighted according to their importance in calculating an earlywood border index, which gives the likelihood of the target vessel's belonging to the earlywood border. If the earlywood border index is above a species-specific threshold, the vessel will be classified as an EBV (fig. 3*d*). Following identification of EBVs, ring pattern–identifying algorithms (fig. 2*c*; third row of table 2) connect EBVs belonging to the same annual ring and thus form continuous borders (fig. 2*b*, 2*e*). All the aforementioned algorithms produce rather coarse results that are subsequently improved by correction algorithms.

Calculation of anatomical parameters. Number, width, and area of annual rings in the secondary root xylem represent the core data output of ROXAS. In addition, data on the area and position of each vessel enable calculation of further anatomical measures. These include vessel density and total and relative vessel area (table 3). All calculated parameter values are automatically saved to an Excel worksheet for further statistical analysis. In addition, the results of vessel extraction and identification of annual rings are visually indicated in the images of the root sections (fig. 3*c*–3*e*).

Species-specific calibration. Forb species, especially those from different families, may be quite distinct in their anatomical patterns (fig. 1; Dietz and Ullmann 1997; Dietz and Schweingruber 2002). Not only the shape, size, and distribution patterns of vessels but also the scaling and the tangential and radial variation of anatomical structures may vary considerably between species (see "Results"). Hence, species-specific calibration is required for morphometric parameters in vessel extraction, for local neighborhood and pattern recognition parameters in EBV detection, and for parameters used in delineation of the earlywood borders (table 2). In

Fig. 3 Process chart of herb-chronology using automated analysis (ROXAS). A sample anatomy (*Penstemon venustus*) is shown in large magnification to visually illustrate the process. Digital images of root cross sections (*a*, *b*) are improved, and xylem vessels are extracted using morphometric parameters (*c*). The innermost vessels of each annual ring (earlywood border vessels [EBVs]; *d*) are identified (see fig. 2*b*) and connected to form annual rings (*e*). Parameters related to plant growth (such as ring width) and functional root anatomy (such as mean vessel area) are automatically calculated and saved to an Excel worksheet. Scale bars = 500 μm.

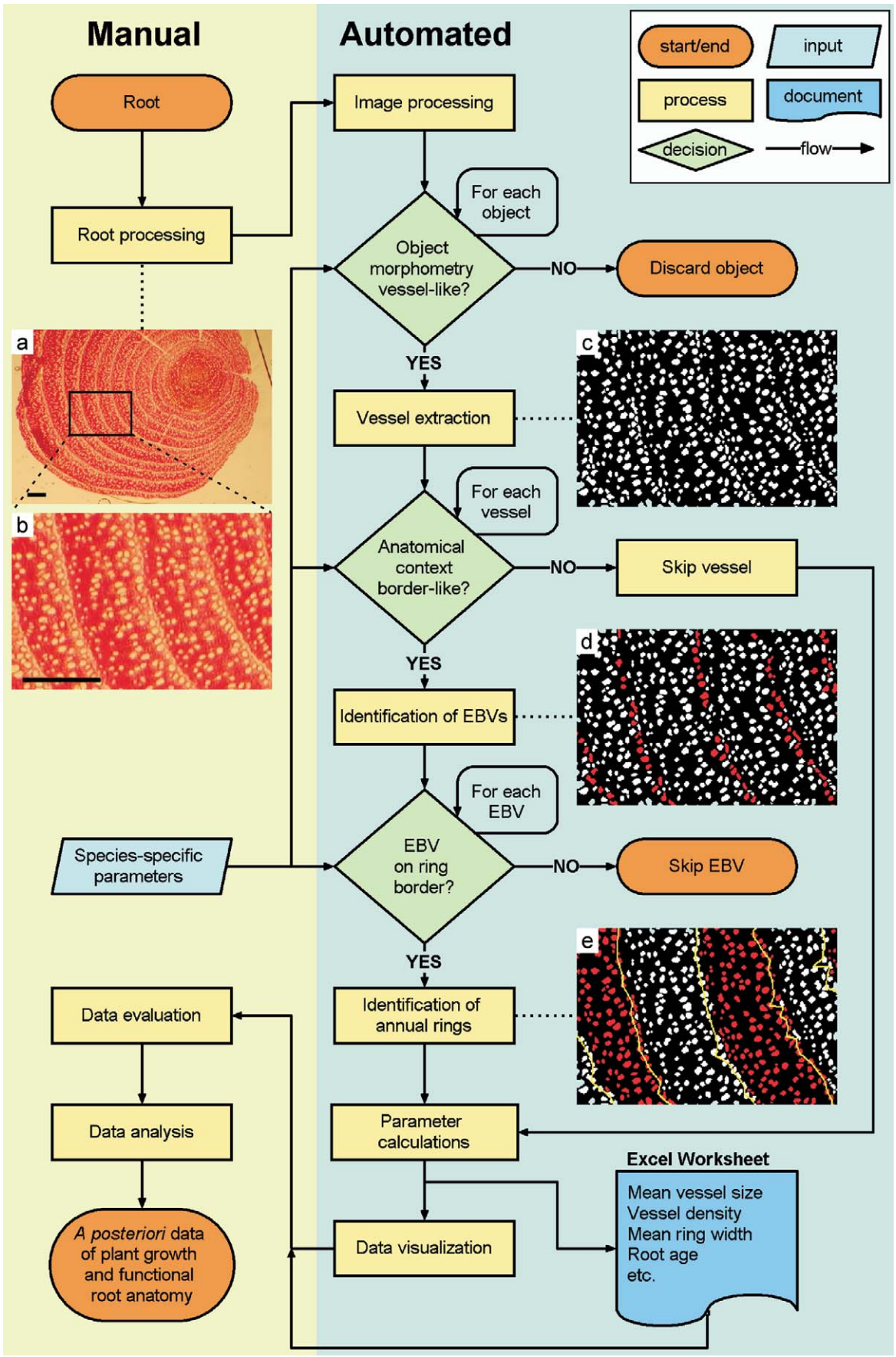
Manual
Automated
start/end
input
process
document
decision
flow
Root
Root processing
Image processing
For each object
Object morphometry vessel-like?
NO
Discard object
YES
Vessel extraction
For each vessel
Anatomical context border-like?
NO
Skip vessel
YES
Identification of EBVs
For each EBV
EBV on ring border?
NO
Skip EBV
YES
Identification of annual rings
Species-specific parameters
Data evaluation
Data analysis
A posteriori data of plant growth and functional root anatomy
Parameter calculations
Data visualization
Excel Worksheet
Mean vessel size
Vessel density
Mean ring width
Root age
etc.
a
b
c
d
e

Table 2

Most Important Morphometric and Pattern Recognition Parameters Used for Species-Specific Calibration

Process	Parameters
Vessel extraction	Object area, roundness, ratio of major to minor axis of object
Identification of EBVs (fig. 2*b*)	Spatial extent of LN window, number of neighboring vessels involved in pattern analysis (only closest neighbors considered), absolute vessel area, relative vessel area (compared to neighboring vessels), radial variation in vessel area, percentage of area occupied by vessel lumina within LN window
Identification of annual rings	Tangential ring watershed, tangential ring vector (see fig. 2*c* for further explanation)

Note. EBV = earlywood border vessel; LN = local neighborhood.

total there are 60 different parameters that can be adjusted to fine-tune automated analysis of annual rings for different forb species, usually taking an experienced observer between 1 and 2 h per species.

Evaluation of the Test Data Set

Vessel extraction and ring identification. After species-specific calibration, the analysis was run on six test individuals per species with unchanged settings. To evaluate the proportion of correctly identified vessels for each cross section (30 in total), a quadratic area that was positioned randomly within the cross section and encompassed 100 vessels indicated by ROXAS was analyzed. Correctly identified vessels, missed vessels, and pseudovessels within this area were determined. Vessels of subpixel size or doubtful vessels were excluded from evaluation. Depending on the species, this fraction ranged from 2% (*Erinus alpinus*) to 28% (*Bunias orientalis*). Likewise, the annual ring borders identified by ROXAS were classified as correct, missed, or pseudo–ring borders. Twenty-three out of ca. 209 true annual ring borders that were not unambiguously discernible by eye because of unclear vessel patterns or were present only in small tangential fractions of the analyzed sector were omitted from analysis.

Accuracy of ring measurements. The results of ring width measurement by automated and manual analysis were compared with those of the reference analysis. In cases where a pseudo–ring border would have led to the omission of both adjoining true rings, these rings were combined and analyzed as one ring to minimize loss of data. A few incompletely identified annual ring borders or annual ring borders that were, in part, too close to each other were excluded from analysis. When data omission or aggregation was necessary (in 41 of 186 annual rings analyzed), the manual and reference data sets were modified accordingly, to maintain consistency.

As a measure of the accuracy of automated and manual ring width measurement, we used the deviation index D, which is the percentage deviation from the reference values:

$$D = \left| \frac{(R - X)}{R} \right| \times 100,$$

where R is the ring width obtained from the reference data set and X is the ring width obtained from either the automated or manual data set. Since D scores were not normally distributed (see fig. 4), median values were used to compare data from manual and automated analysis with those from the reference analysis. The Wilcoxon test was used to assess significance of differences between manual and automated analysis (SAS Institute JMP, ver. 5.1).

Results

The three approaches to measuring annual ring width differed greatly in time efficiency. Irrespective of the species, automated analysis was completed on average in less than 40 s per individual (species-specific calibration not included), whereas manual and reference analysis took an experienced observer more than 4 and 11 min per individual, respectively.

Vessel Extraction and Identification of Annual Rings

Across all species, a total of 2379 true vessels were present within the 30 test areas in the root sections. Almost all true vessels (2321, or 97.6%) were correctly extracted by ROXAS, together with 679 pseudovessels. *Bunias orientalis* was the only species with a noteworthy number of true vessels missed by the extraction procedure (31, or 5%), mainly because of limited resolution in the digital image. Whereas true vessels were well extracted in almost all species, extraction of pseudovessels was mainly restricted to two species, *Erinus alpinus* and *Sanguisorba minor* (table 4).

Of the 186 true annual rings present in all individuals together, 177 (95%) were identified by ROXAS (table 4). Nine (5%) true annual rings were missed, and 17 rings were misidentified (pseudorings). In all species except *E. alpinus* (5 out of 39 annual rings missed), almost all true annual rings were correctly identified.

Accuracy of Ring Width Measurements

Both manual and automated analyses produced ring width measurements of reasonable accuracy, deviating between 2.1% and 5.3% from the reference analysis (fig. 4). In two out of the five species (*B. orientalis* and *Trifolium badium*), ring width measurements by automated analysis tended to be more accurate than those obtained from manual analysis ($P = 0.03$ and 0.11, respectively). In the other species, there were no differences between the two procedures ($P \geq 0.33$). While most measurements deviated only a little from measurements by the reference method ($D \leq 10\%$), ca. 20% of the measurements deviated quite strongly ($D = 10\% - 32\%$) for both methods (fig. 4). There was no significant correlation in the degree of deviation between both methods (Pearson's pairwise correlations, $r = 0.10$, $P = 0.22$), suggesting that error sources differed between the methods. Whereas large deviations ($D \geq 10\%$) were evenly distributed in the central, medium, and peripheral parts of the cross sections in the manual analysis, large deviations were more abundant in

Table 3

Most Important Anatomical Parameters Extracted and Calculated by ROXAS

Parameter	Description
Number of rings (NR)	Number of annual rings
Xylem area (XA)	Area of analyzed secondary xylem within root cross section (fig. 2*a*)
Mean ring width (MRW)	Mean width of an annual ring (fig. 2*a*)
Number of vessels (NV)	Number of vessels within root cross section
Total vessel area (TVA)	Total cross-sectional area of all vessel lumina
Individual vessel area (VA)	Transverse area of individual vessel lumen
Mean vessel area (MVA)	Mean area of all extracted vessels
Vessel density (VD)	Number of vessels per xylem area
Relative vessel area (RVA)	Percentage of area occupied by vessel lumina

Note. The parameters are calculated for each annual ring (except for NR) and for the entire secondary root xylem.

the central and peripheral parts of the cross sections in automated analysis (Pearson's χ^2 test, $P < 0.003$).

Parameters Produced by ROXAS

Here we focus on four main parameters from the set produced by ROXAS (see tables 3, 5): mean ring width, mean vessel area, vessel density, and relative vessel area. There was substantial anatomical variation in all these parameters between the study species (table 5). Mean vessel area ranged from 57 μm^2 (*T. badium*) to 483 μm^2 (*B. orientalis*). Mean ring width ranged from 128 μm (*E. alpinus*) to 880 μm (*B. orientalis*). Conversely, vessel density was very low in *B. orientalis* (55 vessels/mm^2) and very high in *E. alpinus* (768 vessels/mm^2). The relative vessel area ranged from 2.2% (*T. badium*) to 9.5% (*Penstemon venustus*). All four parameters also varied markedly within the study species, the maximum value of each parameter being mostly two to six times larger than the minimum value (compared to four to 14 times for the between-species variation).

Discussion

Our novel approach to measuring anatomical parameters and calculating growth increments in the secondary root xylem of perennial roots using an automated image analysis system (ROXAS) yielded promising results and may represent a useful method for obtaining relevant a posteriori data on plant growth and functional root anatomy. Compared to manual analysis, automated analysis has the advantage of being more time efficient and producing objective, comparable results while identifying and measuring annual rings with sufficient accuracy. Furthermore, ROXAS produces a large set of anatomical measures that were hitherto not easily accessible and that extend the use of herb-chronology beyond plant ecology.

However, there are some constraints and shortcomings in the current implementation of ROXAS. Xylem sectors that are damaged during preparation or do not show coherent annual ring patterns may lead to invalid results. Moreover, success of automated analysis is more dependent on image quality than manual analysis (Spiecker et al. 2000; Soille and Misson 2001). As for manual analysis, tightly packed annual rings cause problems for the ring identification process. In addition, in species with lignified parenchyma cells of about the same size as xylem vessels (e.g., *Erinus alpinus* and *Sanguisorba minor*), parenchyma cells are often insufficiently discriminated from xylem vessels.

Analysis of Annual Growth Increments in the Roots

Almost all true vessels that are clearly visible in the digital images are successfully extracted by ROXAS. Missed vessels predominantly occur when vessels are very small in the digital image (as in *Bunias orientalis*) and/or when there is very poor contrast between vessel walls and vessel lumen (the most problematic vessels in this regard were excluded from analysis, however). Narrow vessels and low contrast can also lead to the identification of a large number of pseudovessels in species where lignified parenchyma and vessel cells are of a similar size (*E. alpinus* and *S. minor*). Although image processing can remedy some image deficiencies, these sometimes have an unfavorable effect on automated (and manual) analysis. Because ROXAS may extract a large number of pseudovessels, some quality control by the user after automated analysis is required. While pseudovessels usually do not impede correct identification of annual rings (pseudovessels are usually narrower than EBVs), they affect the values of other anatomical parameters (see below).

The identification of annual rings by ROXAS is effective in most cases. Failure occurs almost exclusively when

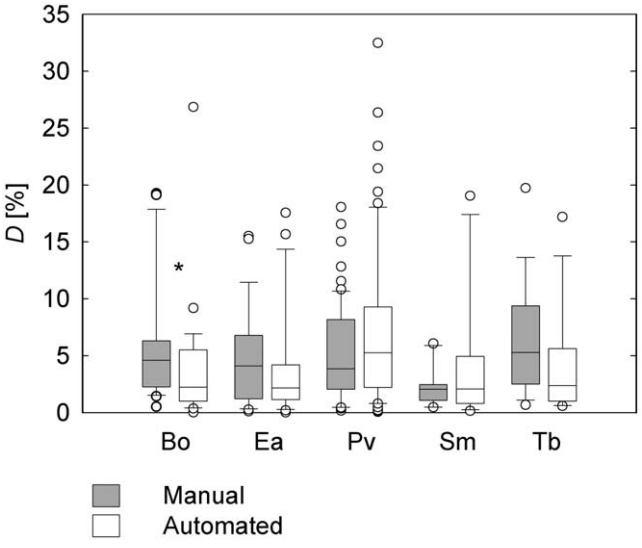

Fig. 4 Accuracy of manual and automated analysis of annual ring width shown as the deviation index *D*, which represents the percentage deviation from the respective reference value. Bo = *Bunias orientalis*, Ea = *Erinus alpinus*, Pv = *Penstemon venustus*, Sm = *Sanguisorba minor*, Tb = *Trifolium badium*. Asterisk denotes $P \leq 0.05$.

Table 4

Accuracy of Vessel Extraction and Identification of Annual Ring Borders by Automated Analysis

	Bunias orientalis	*Erinus alpinus*	*Penstemon venustus*	*Sanguisorba minor*	*Trifolium badium*	Total
Vessel extraction:						
No. true vessels	627	331	563	272	586	2379
No. correctly identified vessels	596	321	555	268	581	2321
No. missed vessels	31	10	8	4	5	58
No. pseudovessels	4	279	45	332	19	679
Identification of annual rings:						
No. true annual rings	31	39	80	18	18	186
No. correctly identified annual rings	31	34	77	17	18	177
No. missed annual rings	0	5	3	1	0	9
No. pseudorings	7	1	2	4	3	17

pseudovessels are the same size as EBVs or when EBVs have not been extracted at all (e.g., in *E. alpinus*). In such cases, the wide pseudovessels interfere with the annual ring pattern and sometimes cause annual rings to be missed. Furthermore, the innermost and outermost annual rings are more often missed by ROXAS than the central annual rings because of an insufficient number of vessels in the local neighborhood for pattern analysis. Missed annual rings can also occur in zones where annual rings are tightly packed because of missing or scarce latewood between earlywood zones. Currently, manually measuring missed annual rings and correcting the data from automated analysis accordingly offers the best way to counter this sort of problem. The main causes of pseudorings are exceptionally wide earlywood zones consisting of consecutive tangential zones of tightly and loosely packed vessels (in some individuals of *B. orientalis* or *S. minor*). However, pseudorings are generally easily detected and can be omitted without invalidating the data because they are just interspersed between true annual rings (in all but one case in our study).

In principle, ring width determination by ROXAS should produce more accurate results than manual analysis because the former first calculates the area of each annual ring and only afterward computes the mean ring width, which is the same approach as in the reference analysis. However, there was only a marginal improvement of accuracy in the automated analysis. On the one hand, this is explained by incomplete identification of annual ring borders. In such cases, ROXAS extrapolates to the outer limits of the specified sector. This extrapolation is a rough estimation, resulting in strongly deviating ring width in a few cases. On the other hand, imperfect identification of EBVs sometimes leads to an oscillating annual ring border, with inaccurate ring width determination as a result. Both types of problems occurred more frequently in the innermost and outermost annual rings, which explains the accumulation of strongly deviating measurements in those regions. Still, in contrast to manual analysis, the accuracy of automated analysis is not dependent on the skills of individual researchers, provided that the same parameter calibration sets are used.

Analysis of Functional Root Anatomy

While parameters related to growth (number of annual rings, mean ring width, area of secondary xylem) may also be obtained relatively easily by manual analysis (Dietz and Fattorini 2002; Dietz et al. 2004; Dietz and von Arx 2005), parameters related to functional root anatomy (e.g., number of vessels, vessel area, and vessel density; table 3) are not directly accessible and require cumbersome manual measuring.

The size of xylem vessels is subject to a trade-off between maximizing conductivity and maintaining the integrity of the water column (Hacke and Sperry 2001) because, within a plant, wide, well-conducting vessels are often more susceptible to drought- or freezing-induced cavitations (Lovisolo and Schubert 1998; Davis et al. 1999; Hacke and Sperry 2001; McElrone et al. 2003). Plants usually control the risk of vessel cavitations by adapting the number and size of their vessels. Adaptation of vessel size can be observed within (temporarily fluctuating growth conditions, different habitats) and between species (Arnold and Mauseth 1999; Gorsuch et al. 2001). The size distribution of vessel

Table 5

Mean Vessel Area (MVA), Mean Ring Width (MRW), Vessel Density (VD), and Relative Vessel Area (RVA) as Produced by Automated Analysis

Parameter	*Bunias orientalis*	*Erinus alpinus*	*Penstemon venustus*	*Sanguisorba minor*	*Trifolium badium*
MVA (μm^2)	483 ± 100	74 ± 8	304 ± 79	189 ± 53	57 ± 13
MRW (μm)	880 ± 254	128 ± 30	258 ± 57	872 ± 513	239 ± 88
VD (vessels/mm^2)	55 ± 38	768 ± 213	307 ± 55	454 ± 273	389 ± 200
RVA (%)	2.68 ± 1.66	5.69 ± 1.81	9.52 ± 3.49	7.60 ± 2.53	2.21 ± 1.42

Note. The values shown are means of six plants per species ± 1 SD.

populations within a plant is also a crucial characteristic, since it determines how many vessels remain functional after losing a certain amount of conducting capacity (Mauseth and Stevenson 2004; Stevenson and Mauseth 2004).

Our study species exhibited large variation in parameters related to both growth and functional root anatomy that may be specific to a given species or environment. Measures of individual and relative vessel area and vessel density obtained by ROXAS are consistent in their data range with results from other studies (Arnold and Mauseth 1999; Davis et al. 1999; Gorsuch et al. 2001; Solla and Gil 2002; Lens et al. 2004; Stevenson and Mauseth 2004). Whereas all these studies used only vessel diameter, deduced vessel area from a few vessel diameters, or included only a subset of all vessels, with our automated approach we were able to quantitatively measure all vessels within the secondary root xylem. The accuracy of the obtained values is affected only by the quality of vessel extraction. In species that produce a significant number of pseudovessels, these may have an effect on total and relative vessel area. However, this effect is usually minor, except for the few species where pseudovessels are of the same size as EBVs (e.g., *E. alpinus* but not *S. minor*).

Additional Approaches Using Automated Herb-Chronological Analysis

A better understanding of the significance of concerted effects of variation in distinct characteristics, such as plant growth and functional anatomy, on the basis of automated herb-chronology meets the need for a broad integrative approach in plant ecology (Novoplansky 2002). Such a broad approach may address responses in plant growth and development at different levels of resolution. Mean parameter values of species may allow interspecific comparisons of general adaptive strategies, whereas year- and site-specific data within species give insight into individual life histories and plastic responses to environmental fluctuations. For example, forbs growing at higher latitudes or altitudes may form rather narrow annual rings (table 5) because of more restrictive growth conditions and, to prevent freezing-induced cavitation, a comparatively high proportion of narrow vessels (Lens et al. 2004). In a particularly wet year, a species growing in a dry habitat may develop relatively wide annual rings (Dietz and von Arx 2005) and wider vessels but lower vessel density and smaller relative vessel area, which would improve water transport efficiency, because allocation to water transport structures is less crucial under such atypical conditions (Solla and Gil 2002; Stevenson and Mauseth 2004). Fluctuations in annual ring characteristics may also help to identify and evaluate switches in phenological stages of established plants. For example, reproductive effort during flowering years may have a discernible effect on the radial growth of annual rings or vessel-related characteristics compared to years when plants do not flower. In this case, questions about changes in the life history of species, for instance, upon introduction into a new area, may be tackled (Müller-Schärer et al. 2004).

Further Development of ROXAS

Suboptimal performance of ROXAS (and other pattern analysis systems) results from the fact that when dealing with natural phenomena it is impossible to account for all peculiarities that may occur in the patterns (Conner et al. 2000). Although there is still potential to further improve the algorithms of image processing, vessel extraction, and pattern recognition in ROXAS, it will be more efficient to focus on implementation of tools that allow the analyst to actively adapt and correct the results of automated image analysis in an advanced future version of ROXAS (see Conner et al. 2000). Information on future developments of the system and availability for researchers will be published on the herb-chronology web pages (Dietz and von Arx 2004).

Acknowledgments

We thank Lea Wirth for providing us with the images of *Erinus alpinus* root sections. Silke Dietz helped us in the field. Catherine Parks provided us with lab space and information on the Wallowa Mountains. We thank Moritz Kuhn for valuable discussions on several algorithms in ROXAS. Jake M. Alexander, James D. Mauseth, and an anonymous reviewer improved a former version of the manuscript. This work was supported by a grant of the Swiss National Science Foundation to H. Dietz (NF 31-65426.01).

Literature Cited

Arnold DH, JD Mauseth 1999 Effects of environmental factors on development of wood. Am J Bot 86:367–371.

Boggs KW, JM Story 1987 The population age structure of spotted knapweed (*Centaurea maculosa*) in Montana. Weed Sci 35: 194–198.

Carlquist S 2001 Comparative wood anatomy: systematic, ecological, and evolutionary aspects of dicotyledon wood. 2nd ed. Springer, Berlin. 448 pp.

Conner WS, RA Schowengerdt, M Munro, MK Hughes 2000 Engineering design of an image acquisition and analysis system for dendrochronology. Opt Eng 39:453–463.

Davis SD, JS Sperry, UG Hacke 1999 The relationship between xylem conduit diameter and cavitation caused by freezing. Am J Bot 86:1367–1372.

Dietz H, M Fattorini 2002 Comparative analysis of growth rings in perennial forbs grown in an alpine restoration experiment. Ann Bot 90:663–668.

Dietz H, FH Schweingruber 2002 Annual rings in native and introduced forbs of lower Michigan, USA. Can J Bot 80:642–649.

Dietz H, I Ullmann 1997 Age-determination of dicotyledonous herbaceous perennials by means of annual rings: exception or rule? Ann Bot 80:377–379.

——— 1998 Ecological application of "herbchronology": comparative stand age structure analyses of the invasive plant *Bunias orientalis* L. Ann Bot 82:471–480.

Dietz H, G von Arx 2004 Geobotanical Institute ETH research spotlight: herb-chronology. http://www.geobot.ethz.ch/spotlights/herbchronology.

——— 2005 Climatic fluctuation causes large-scale synchronous variation in radial root increments of perennial forbs. Ecology 86: 327–333.

Dietz H, G von Arx, S Dietz 2004 Growth patterns in two alpine forbs as preserved in annual rings of the roots: the influence of a snowbank gradient. Arct Alp Res 36:591–597.

Gorsuch DM, SF Oberbauer, JB Fisher 2001 Comparative vessel anatomy of arctic deciduous and evergreen dicots. Am J Bot 88: 1643–1649.

Grissino-Mayer HD 1996 Ultimate tree-ring Web pages. http://web.utk.edu/~grissino.

Grissino-Mayer HD, HC Fritts 1997 The International Tree-Ring Data Bank: an enhanced global database serving the global scientific community. Holocene 7:235–238.

Hacke UG, JS Sperry 2001 Functional and ecological xylem anatomy. Perspect Plant Ecol Evol Syst 4:97–115.

Harper JL 1977 Population biology of plants. Academic Press, London. 892 pp.

Humulum C 1981 Age distribution and fertility of populations of the arctic-alpine species *Oxyria digyna*. Holarct Ecol 4:238–244.

Lens F, JL Luteyn, E Smets, S Jansen 2004 Ecological trends in the wood anatomy of Vaccinioideae (Ericaceae s.l.). Flora 199: 309–319.

Lovisolo C, A Schubert 1998 Effects of water stress on vessel size and xylem hydraulic conductivity in *Vitis vinifera* L. J Exp Bot 49: 693–700.

Mauseth JD, JF Stevenson 2004 Theoretical considerations of vessel diameter and conductive safety in populations of vessels. Int J Plant Sci 165:359–368.

McElrone AJ, JL Sherald, IN Forseth 2003 Interactive effects of water stress and xylem-limited bacterial infection on the water relations of a host vine. J Exp Bot 54:419–430.

Media Cybernetics 2001 Image-Pro Plus reference guide for Windows. Media Cybernetics, Silver Spring, MD. 746 pp.

Müller-Schärer H, U Schaffner, T Steinger 2004 Evolution in invasive plants: implications for biological control. Trends Ecol Evol 19: 417–422.

Novoplansky A 2002 Developmental plasticity in plants: implications of non-cognitive behavior. Evol Ecol 16:177–188.

Rabotnov TA 1960 Methods of determining the age and length of life of herbaceous plants. Field Geobot 2:249–262.

Roach DA 2003 Age-specific demography in *Plantago*: variation among cohorts in a natural plant population. Ecology 84:749–756.

Russ JC 2002 The image processing handbook. 4th ed. CRC, Boca Raton, FL. 732 pp.

Soille P, L Misson 2001 Tree ring area measurements using morphological image analysis. Can J For Res 31:1074–1083.

Solla A, L Gil 2002 Xylem vessel diameter as a factor in resistance of *Ulmus minor* to *Ophiostoma novo-ulmi*. For Pathol 32:123–134.

Spiecker H, MG Schinker, J Hansen, Y Park, T Ebding, W Döll 2000 Cell structure in tree rings: novel methods for preparation and image analysis of large cross sections. IAWA J 21: 261–273.

Stevenson JF, JD Mauseth 2004 Effects of environment on vessel characters in cactus wood. Int J Plant Sci 165:347–357.

Werner PA 1978 On the determination of age in *Liatris aspera* using cross-sections of corms: implications for past demographic studies. Am Nat 112:1113–1120.